The Leading Proton Spectrometer of ZEUS

Design, construction and performance

Roberto Sacchi
Università di Torino
ZEUS collaboration

HERA-LHC Workshop, March 26-27, 2004

1. **Introduction**
2. **The Leading Proton Spectrometer:**
   - **beam optics and general layout**
   - **electronics and mechanics**
   - **detector performance**
   - **alignment and calibration**
   - **analysis techniques**
3. **Conclusions**

THE LPS GROUP

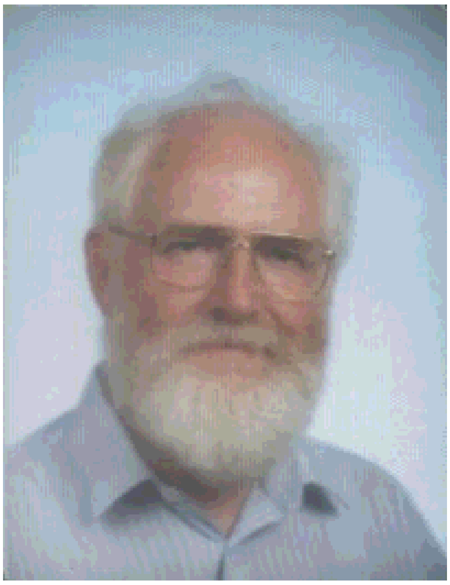

[1]G.Anzivino [6]M.Arneodo [4]R.Ayad [5]R.Baldo [3]E.Barberis [5]F.Benotto [3]N.Cartiglia [6]M.Capua [4]M.Chiarini [5]R.Cirio [5]M.Costa [3]J.De Witt [5]E.Debe' [3]D.E.Dorfan [3]T.Dubbs [5]G.Dughera [5]M.I.Ferrero [5]C.Ferrero [2]P.Ford [4]I.Gialas [6]A.Garfagnini [5]G.Giraudo [3]A.Grillo [2]M.Hourican [3]B.Hubbard [6]L.Iannotti [5]P.Isoardi [5]L.Lamberti [2]H.Larsen [3]A.Litke [3]W.Lockman [5]A.Manara [5]S.Maselli [5]V.Monaco [5]F.Morrone [3]J.Ng [1]T.Massam [5]M.Massazza [5]V.Monaco [2]C.Nemoz [3]K.O'Shaughnessy [5]R.Parena [5]E.Pernigotti [5]C.Peroni [5]M.C.Petrucci D.Pitzl [3]J.Rahn [3]W.A.Rowe [5]M.Ruspa [5]R.Sacchi [3]H.F.-W.Sadrozinski [5]A.Solano [2]J.Schipper [3]A.Seiden [3]E.Spencer [5]A.Staiano [5]P.P.Trapani [1]M.Veltri [5]D.Veniali [3]A.Webster [3]M.Wilder [3]R.Wichmann [3]D.Williams [4]Y.Zamora [5]A.Zampieri [3]D.Zer Zion and [124]A.Zichichi.

(1) University/INFN Bologna, (2) LAA at CERN Geneve, (3) University of Santa Cruz, (4) Worldlab Lausanne, (5) University/INFN Torino, (6) University Calabria /INFN Cosenza.

Forward physics at HERA

Large fraction of e–p interactions produces leading baryons.

- **peripheral processes**
- **small $t = (p - p')^2$**
- **broad $x_L = p'/p$ spectrum**

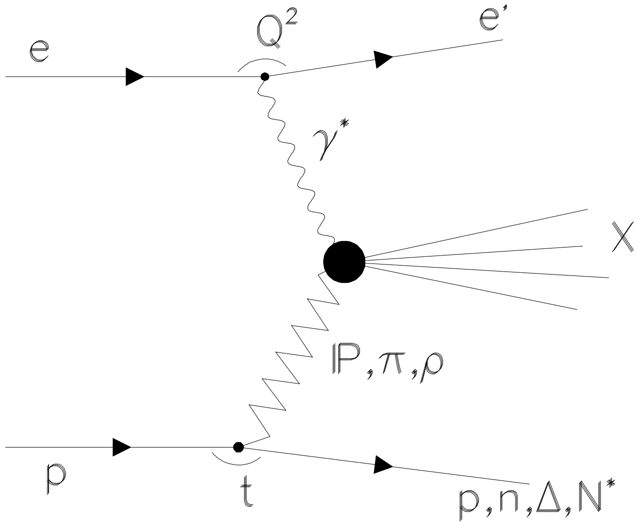

- **If the proton is detected:**
  - ⇒ **elastic and diffractive scattering**
  - ⇒ **factorization, one particle exchange models**
  - ⇒ **target fragmentation in non-diffractive DIS**
  - ⇒ **measurement of M_X**
- **If neutron is detected (charged exchange):**
  - ⇒ **total $\gamma\pi$ cross section**
  - ⇒ **pion structure function**

The ZEUS detector has been equipped with both a Leading Proton Spectrometer (LPS) and a Forward Neutron Calorimeter (FNC).

Proton tagging: technical skills

- Design spectrometer to fit in with HERA maximizing the acceptance;
- make large shaped detectors fitting closely to the elliptically-shaped beam;
- develop application-specific front-end electronics working very near to high intensity and high energy beam;
- solve cooling and RF shielding problems;
- develop system capable of retracting detectors during beam fill and automatically re-install them during luminosity;
- develop safety system to protect against detector damage;
- develop reconstruction and calibration method.

The beam optics (pre-HERA lumi upgrade)

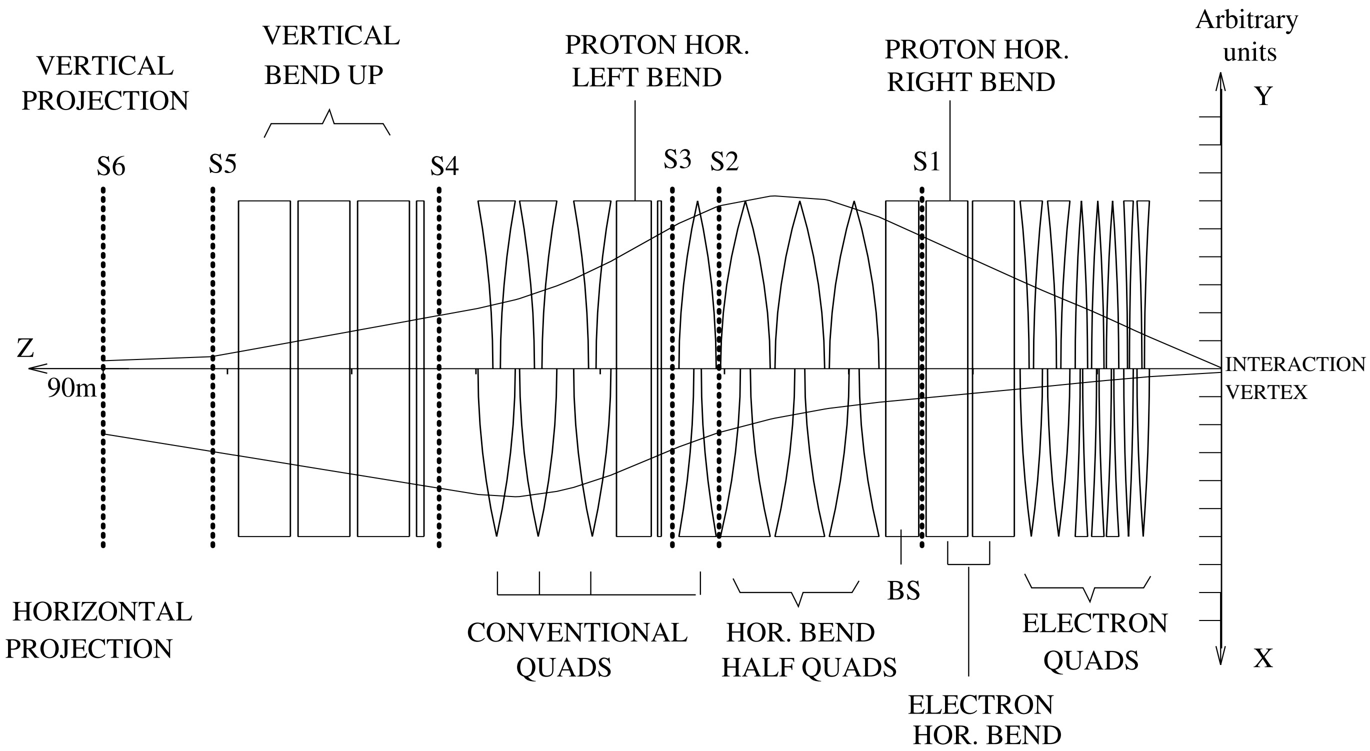

At the interaction point:

$$\beta_x^* = 7m \implies \sigma_{p_x} = \mathbf{45\ MeV}$$
$$\beta_y^* = 0.7m \implies \sigma_{p_y} = \mathbf{100\ MeV}$$

The curves represent the horizontal and vertical projections of the 10σ envelope of the beam.

Not shown: <u>beam position monitors</u> close to stations S3 and S4.

The Leading Proton Spectrometer

(INFN Bologna, INFN Torino, UCSC)

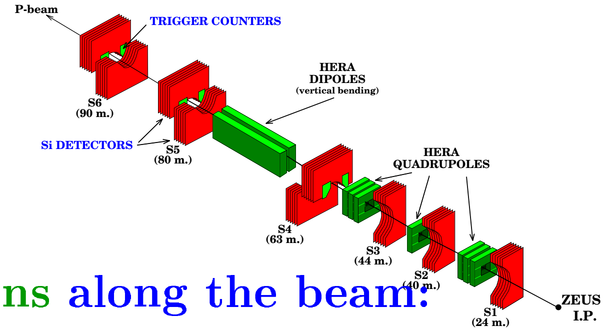

- **Six detector stations along the beam:**
  S1 $\longrightarrow$ S3 single "lateral" stations
  S4 $\longrightarrow$ S6 double "vertical" stations

- **Detector operations using Roman pots**

- **Six single-sided μstrip silicon detectors per pot:**

  - **three different strip orientations** $(0^o, +45^o, -45^o)$
    pitch: $115\mu m \rightarrow 0^o$
    $115/\sqrt{2}\mu m \rightarrow \pm 45^o$
  - **elliptical shaped cut follows the** $10\ \sigma$ **beam profile.**

- **Trigger system for diffractive events (installed in 1995)**

- **TOTAL:** $\Rightarrow$ **60 detector planes**
  $\Rightarrow \sim$ **54000 readout channels**

The LPS detectors

- 300 μm thick single-sided μstrip silicon planes;
- up to 1024 p+ strips implanted on n+ substrate;
- varying sizes (approx 6×4 cm^2) and elliptical cuts;
- 3 manifacturers CANBERRA, EURYSIS, MICRON, using different cut technologies;
- all produced planes carefully tested before mounting.

Results

Yield ~ 85%
Depletion voltage 35÷50 V
Strip capacitance
~ 1.2 pF/cm
Leakage current
few nA per strip
Precision on cutout better than 100 μm

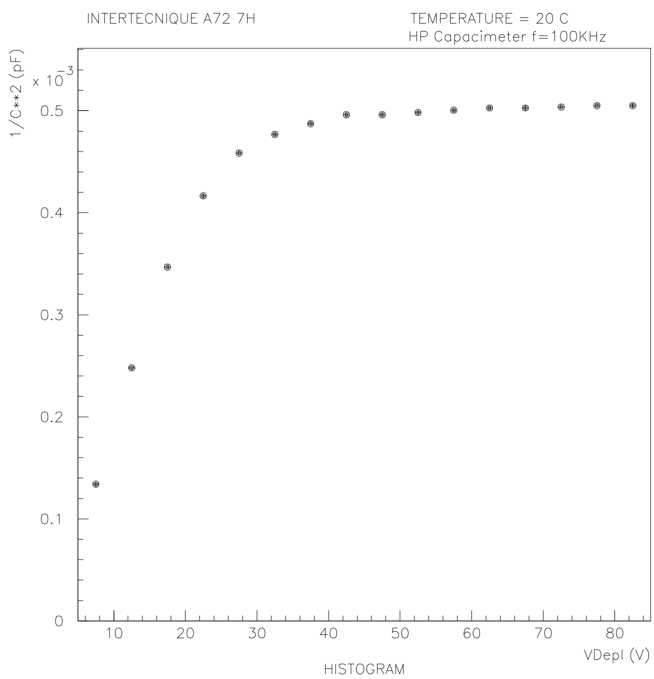

The LPS FE electronics

TEXZ VLSI bipolar chip

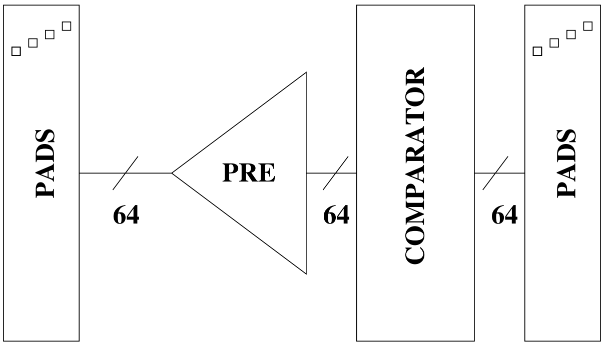

DC Coupled to the detector
Shaping time τ_s= **32 nsec**
Gain 150±20 mV/fC
S/N 22.3 with input load **11pF**
σ_n= **690 + 40C** [e$^-$]
Power 2 mW/channel

DTSC VLSI CMOS chip

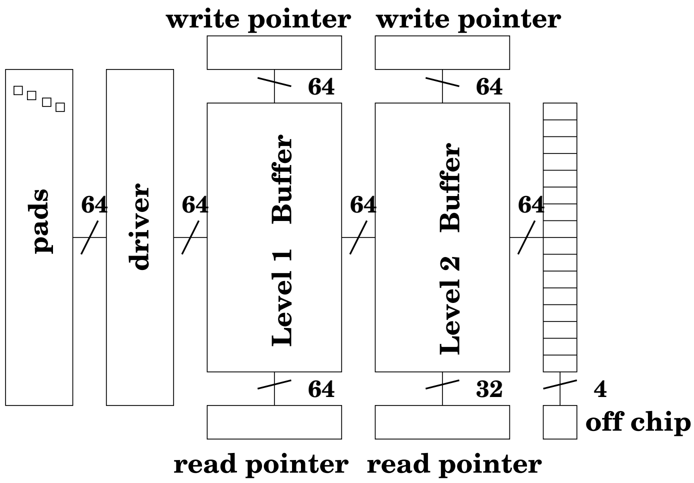

Directly coupled to TEXZ
Clock cycle 10 MHz
2 level buffers
FLT pipeline 5 μsec lenght
Power 2 mW/channel

Radiation hardness of both chips tested up to doses of 5 Mrad and fluences of $1.1 \cdot 10^{14}$ p/cm.

Detector and FE chips mounted on a 6 layers Cu-Invar support, with SMD filters on bias lines. Water cooling with 1 mm^2 pipe glued on multilayer support (45^{o}C → 24^{o}C).

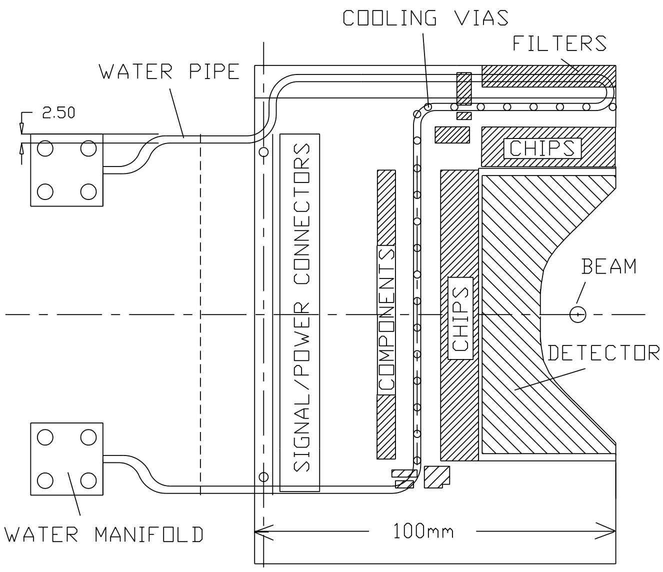

The LPS First Level Trigger

S4-S5-S6 Spectrometer → elastic/diffractive events

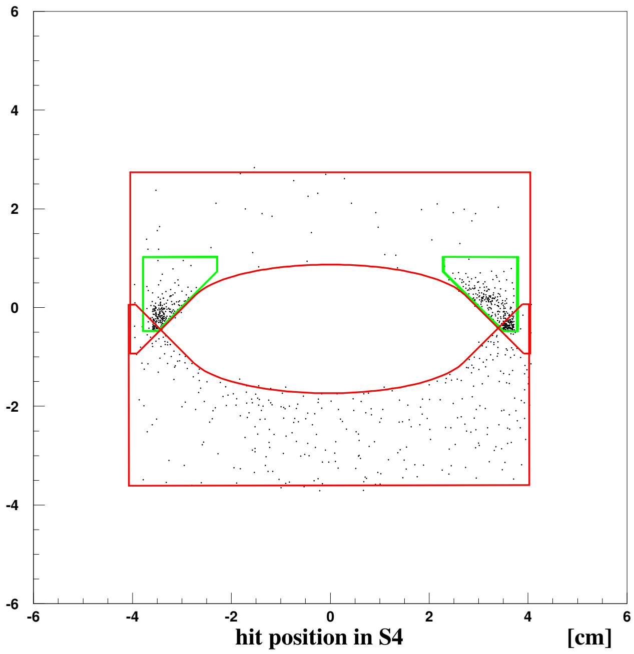

Diffractive cross section peaks at $\frac{p'}{p} = x_L = 1$, in the detector edges.

Trigger detectors shapes modelled to have efficiency $\geq 50\%$ for $x_L \geq 0.95$ and $\sim 100\%$ for $x_L = 1.0$.

AC detectors segmented in 20 strips (750μ**m** pitch, **2** orientations, x-y) in order to tag track correlations with coincidence matrices (FPGA units).

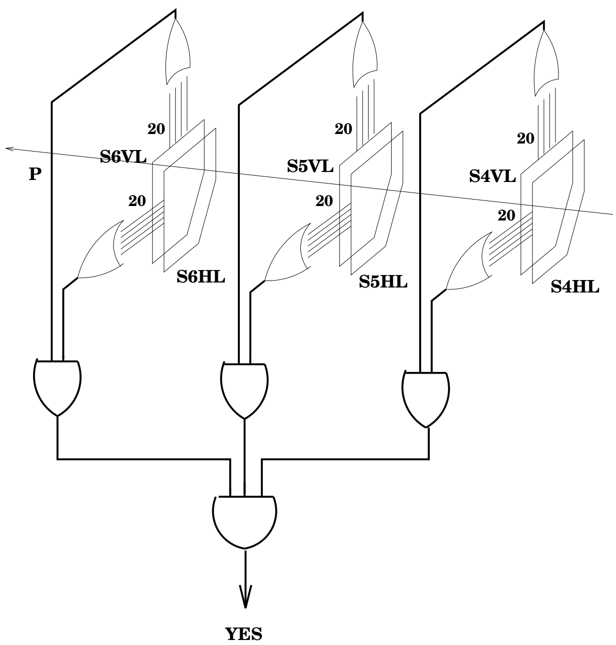

Trigger logic:
No Momentum Cut trigger. Typical data taking standalone rate $\sim$ **2 kHz** with good beam conditions.

Real trigger efficiency very much dependent on detector and beam positions ⟹ large systematic uncertainty

ROMAN POTS OPERATIONS

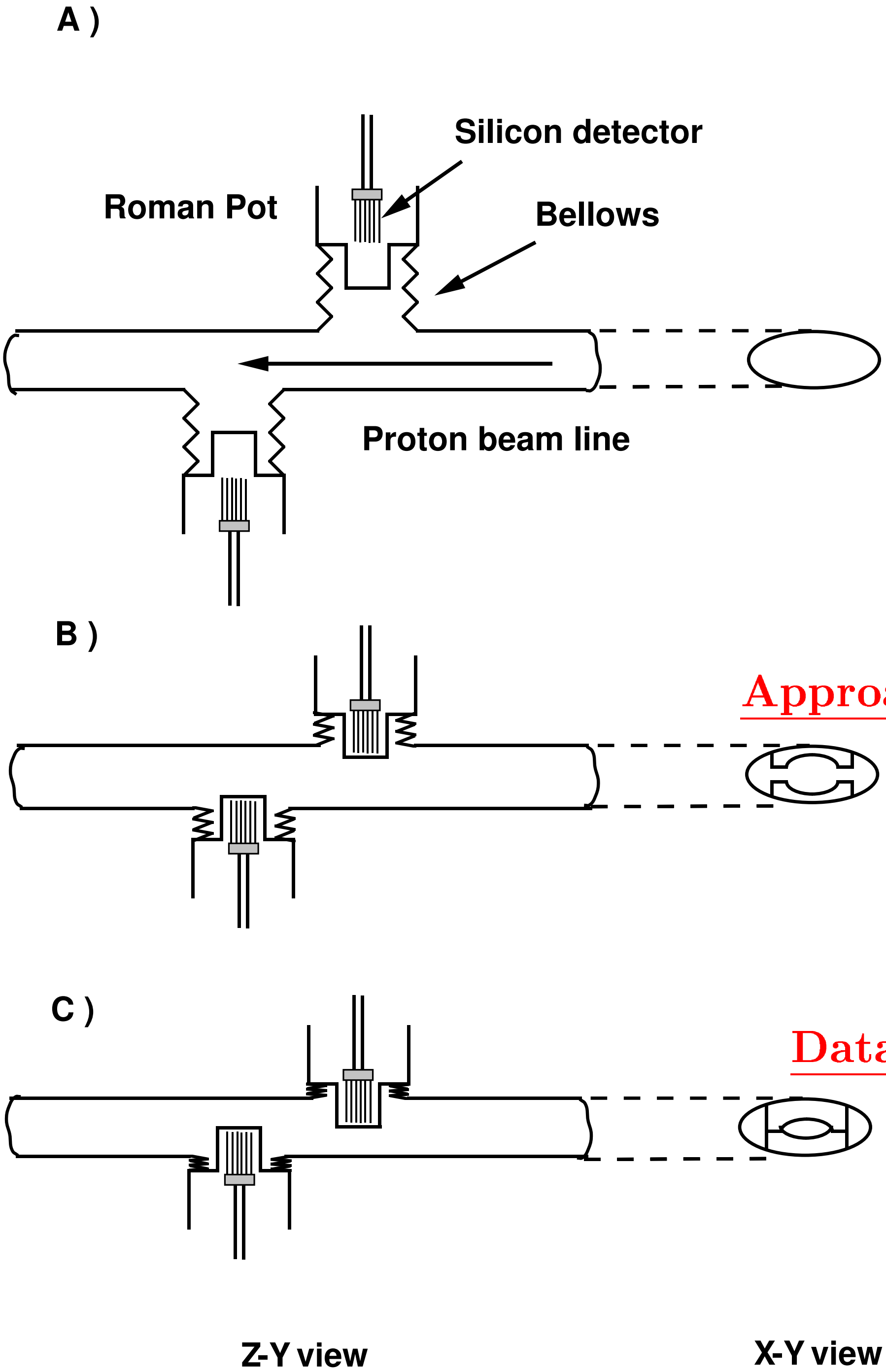

Hera filling

Approaching the beam

Data taking position

In data taking position, the detector edges are only few millimeters from 1 MJ of stored proton beam !

Mechanical construction

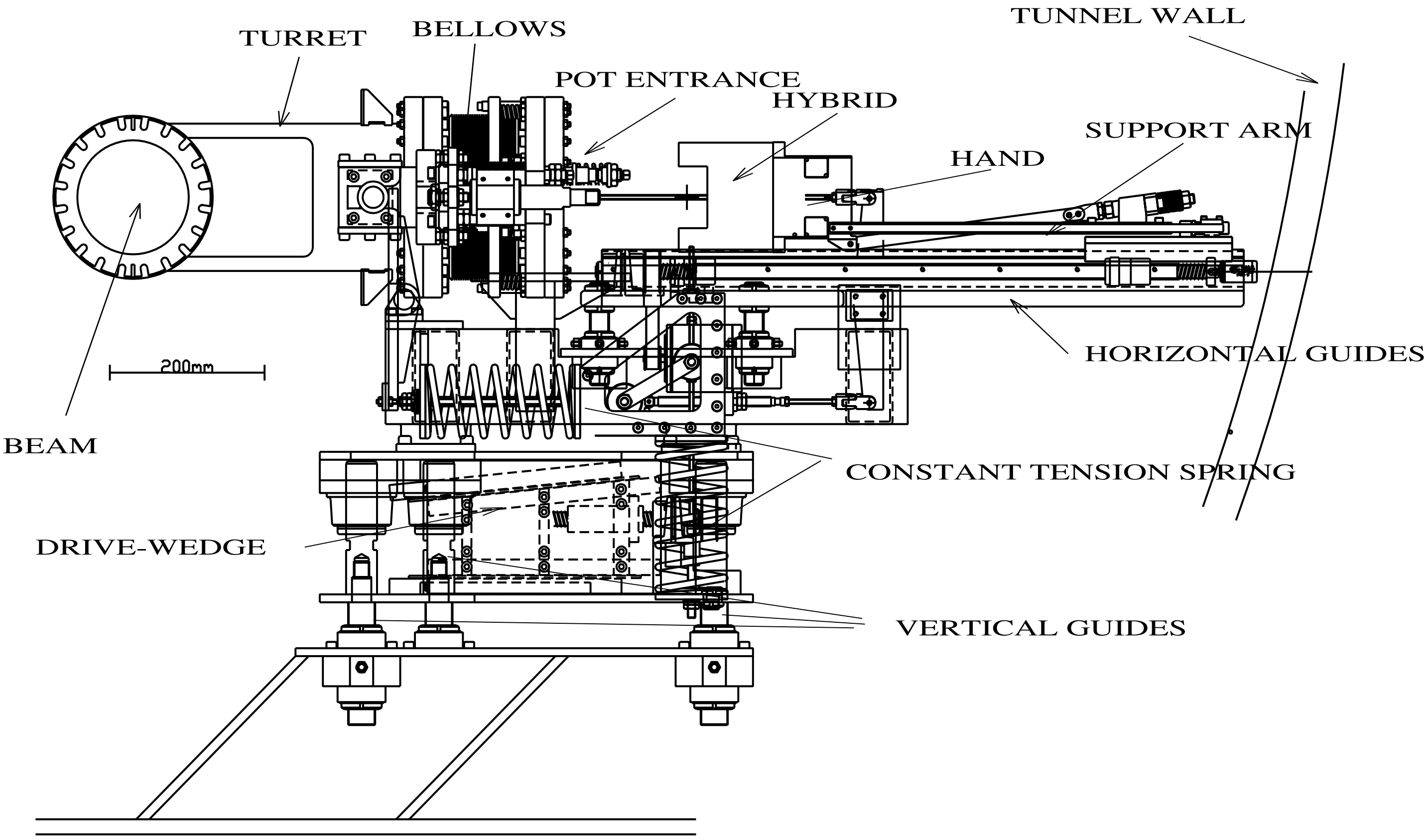

- **Roman Pots:** 3 mm thick with thin window (380 μm)
  $\Rightarrow$ Vacuum sealed by welded bellows.
- **Three movements:**
  1) Detector insertion in pot
  2) In/Out pot displacement (bellow compression)
  3) Transverse pot displacement
     $\Rightarrow$ station displacement (S1$\rightarrow$S4)
     $\Rightarrow$ bellow tilt (S5,S6)
- **Position measurement:**
  resolvers $\sigma \sim 5\mu$m
  linear trasducers $\sigma \sim 25\mu$m (mov. 2, stations S5,S6)
- **Vacuum force compensation:** (Vacuum force $\sim$ 8kN)
  mechanic system (S1$\rightarrow$S4)
  pneumatic system (S5,S6)

The LPS Data Taking operations

LPS moved with an automatic movement procedure by the shift crew at the beginning of each fill.
Monitor:

1. **LPS trigger rate**
2. **FNC trigger rate**
3. **LPS Beam loss monitors**
4. **HERA p-collimator pos./rates**
5. **HERA BPM**

Two alarm threshold levels:
low thresh.:ALARM = set LPS movement in wait condition;
high thresh.:PANIC = generate a fast extraction of the pots.

Time required to fully position the spectrometer $\sim$ 25 minutes.

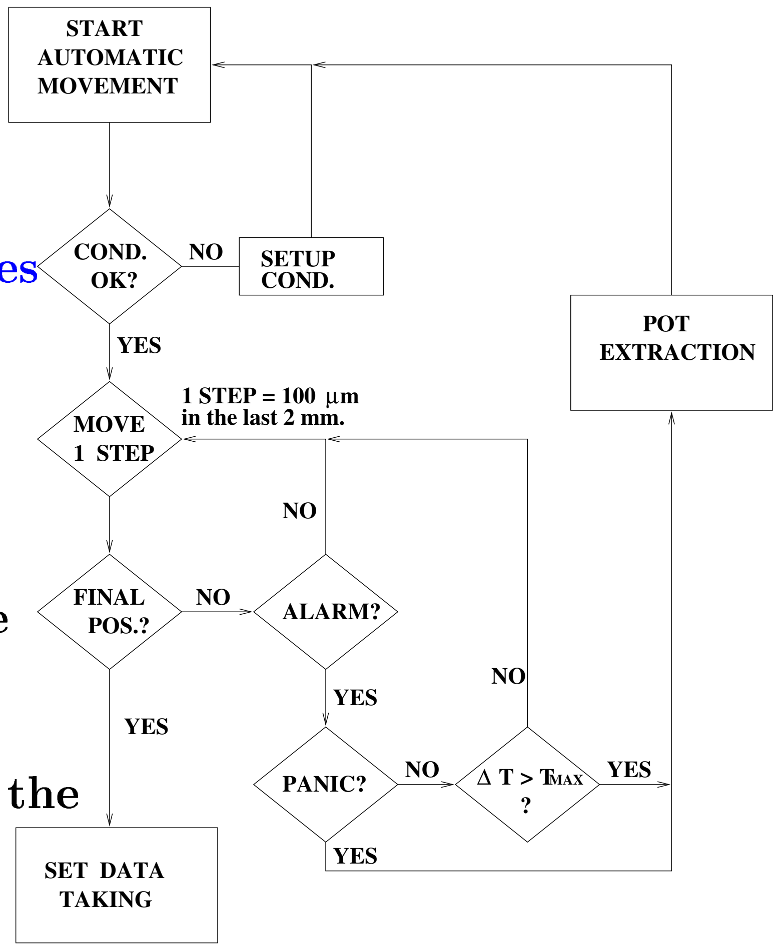

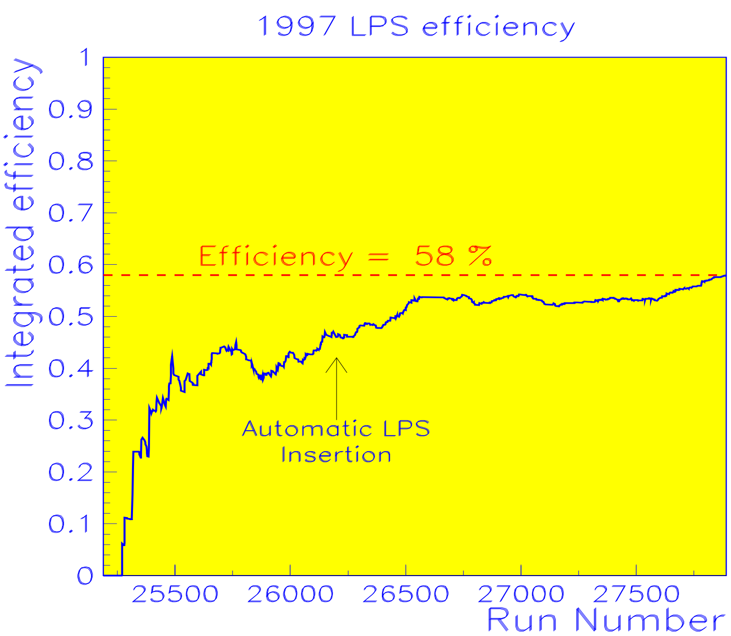

Detector Performance

Integrated luminosity collected by ZEUS and by the LPS (the column marked with an asterisk is the luminosity which is used in physics analyses):

	Luminosity (pb^{-1})				Luminosity (pb^{-1})		
Year	ZEUS	LPS	LPS*	Year	ZEUS	LPS	LPS*
1994	3.0	0.9	0.9	1997	28	14	13
1995	6.6	3.5	3.4	1999	36	15	10
1996	11	4.0	0.0	2000	47	35	35
Total					132	72	62

The inefficiency was mainly caused by bad HERA beam conditions and (in)compatibility with HERA-B wire target.

LPS problems leading to negligible loss of data:

- ⇒ mechanical problems with pot insertion;
- ⇒ problems of cooling system.

Few planes showed problems of increased leakage current or dead DTSC (mechanical stress and effects of radiation):

- ⇒ planes replaced during machine shutdown;
- ⇒ no impact on efficiency in s4-s5-s6;
- ⇒ degrade performance of s1-s2-s3 (year 2000).

Excluding malfunctioning planes:

- ⇒ noisy or dead channels $< 2\%$;
- ⇒ measured plane efficiency $> 99.5\%$;
- ⇒ average noise < 0.3 channels/plane firing per bunch crossing

Simplified beam optics

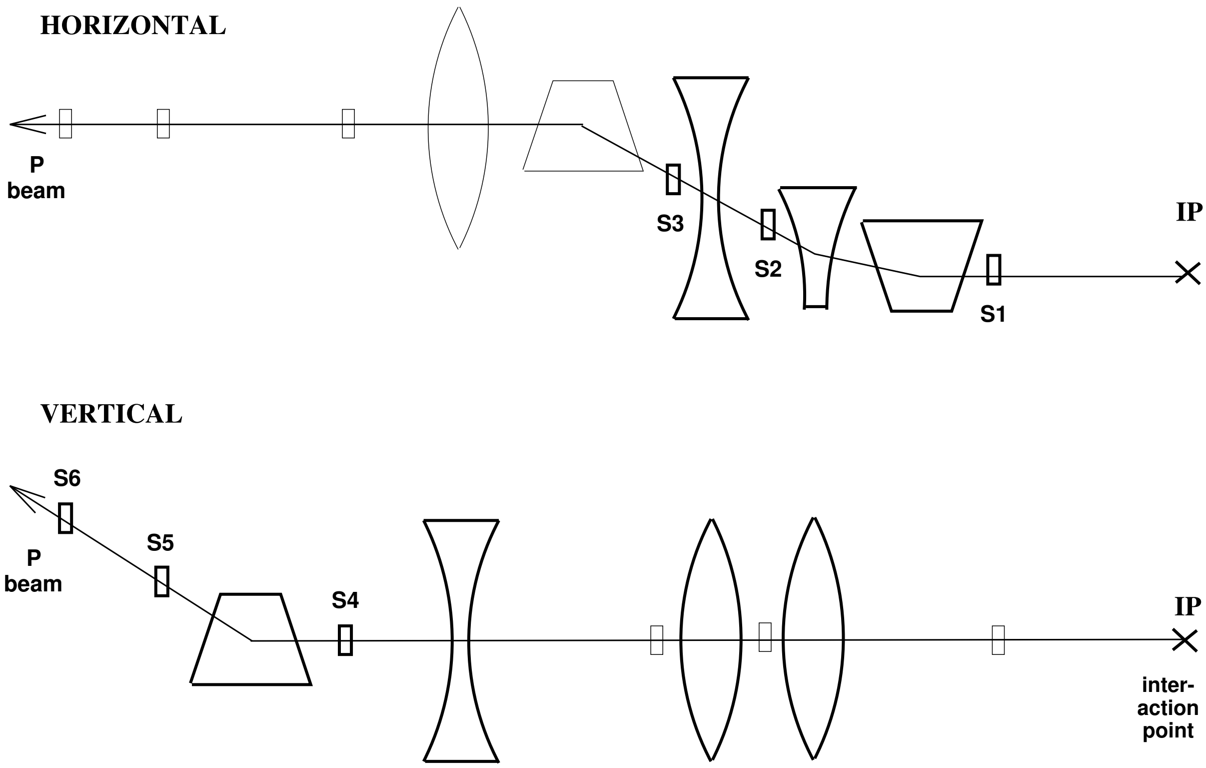

- **Two independent spectrometers, S1-S2-S3 and S4-S5-S6, with almost no acceptance overlap**
- **Momentum measured through the beam optics elements**

Note:

- 3-station tracks (e.g. S4-S5-S6)
  $\Rightarrow$ simple case
- Method developed for 2-station tracks
  $\Rightarrow$ use the vertex as third point
  $\Rightarrow$ maximize the acceptance

The LPS Reconstruction

The LPS pattern recognition proceeds through the following steps:

1. noisy channel suppression;
2. combination of clusters in each planes to fit track segments in each station (coordinates);
3. combination of pairs of coordinates belonging to different stations into 2-station track candidates;
4. combination of 2-station track candidates in 3-station tracks.

coordinate reconstruction

Coordinate quality is classified according to quality codes related to the probability that the reconstructed coordinate belongs to a track rather than to combinatorial background.

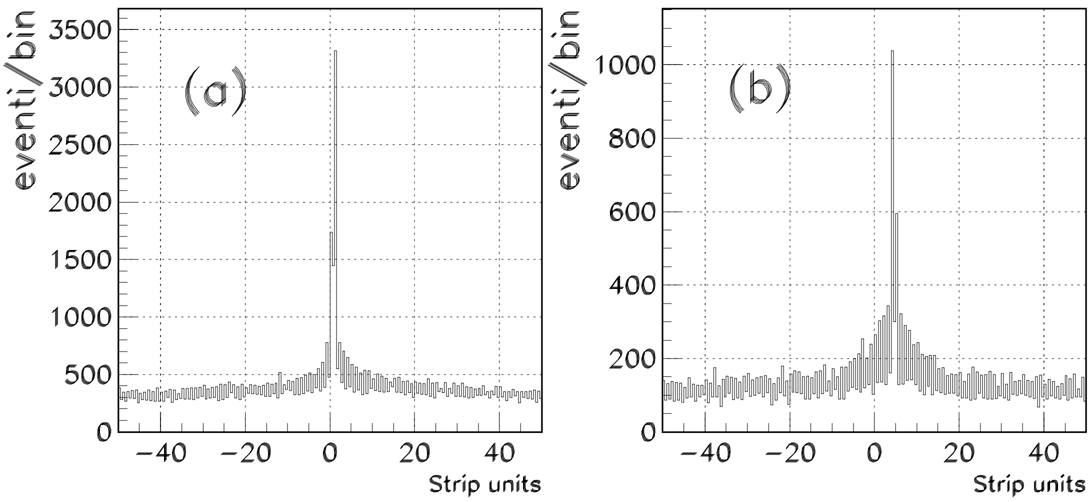

6 planes, 3 views in each pot:

Quality Code	Type	Quality Code	Type
1	\\\||//	4	\\\|/
2	\\\||/	5	\\\|
3	\\\||	6	\\|/
		7	\\|

The LPS Reconstruction

Reconstructed coordinates

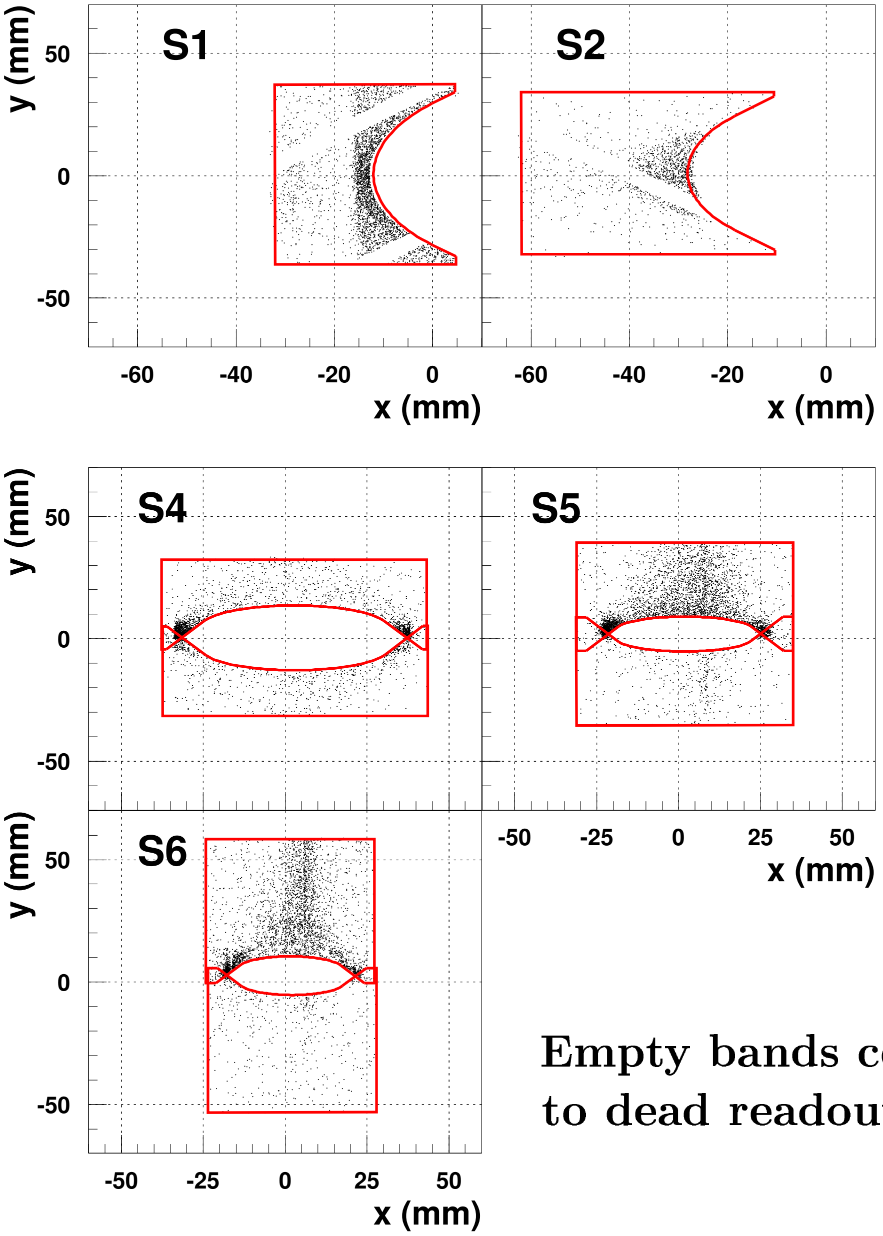

Empty bands correspond to dead readout chips.

Resolution:	$\sim 20\ \mu m \oplus 10\ \mu m$ (S1 $\Rightarrow$ S4)
	$\sim 20\ \mu m \oplus 30\ \mu m$ (S5, S6)
Dead channels	$\lesssim 2\ \%$
Noise	$0.2 \div 0.3$ cluster/event in each plane

The LPS Reconstruction

Two stations correlations

The beam optics is described by a linear beam transport equation (beam reference system). It relates (x_a, x'_a) (position and angle) at a given z to (x_a, x'_a)at $z = 0$.

$$\begin{pmatrix} x_a \\ x'_a \end{pmatrix}_{z=z_a} = \begin{pmatrix} T^a_{11}(x_L) & T^a_{12}(x_L) \\ T^a_{21}(x_L) & T^a_{22}(x_L) \end{pmatrix} \begin{pmatrix} x_0 \\ x'_0 \end{pmatrix}_{z=0} + \begin{pmatrix} B^a_1(x_L) \\ B^a_2(x_L) \end{pmatrix} \quad (1)$$

The transport matrix $\mathbf{T}^a$, function of the longitudinal momentum of the track, describes the effect of the beam quadrupoles. The vector $\mathbf{B}^a$ describes bending effect (dipoles and off axis quadrupoles).

Solving eq. ?? for two stations (a,b), one can obtain the two independent linear equations:

$$\begin{array}{rcl} x_b & = & m^{ab}_x(x_L)x_a + c^{ab}_x(x_L, x_0) \\ y_b & = & m^{ab}_y(x_L)y_a + c^{ab}_y(x_L, y_0) \end{array} \quad (2)$$

TRACKS AT FIXED MOMENTUM ARE LINEARLY CORRELATED IN THEIR X AND Y POSITIONS IN PAIRS OF STATIONS

The LPS Reconstruction

x projection:
low resolution,
no ambiguity

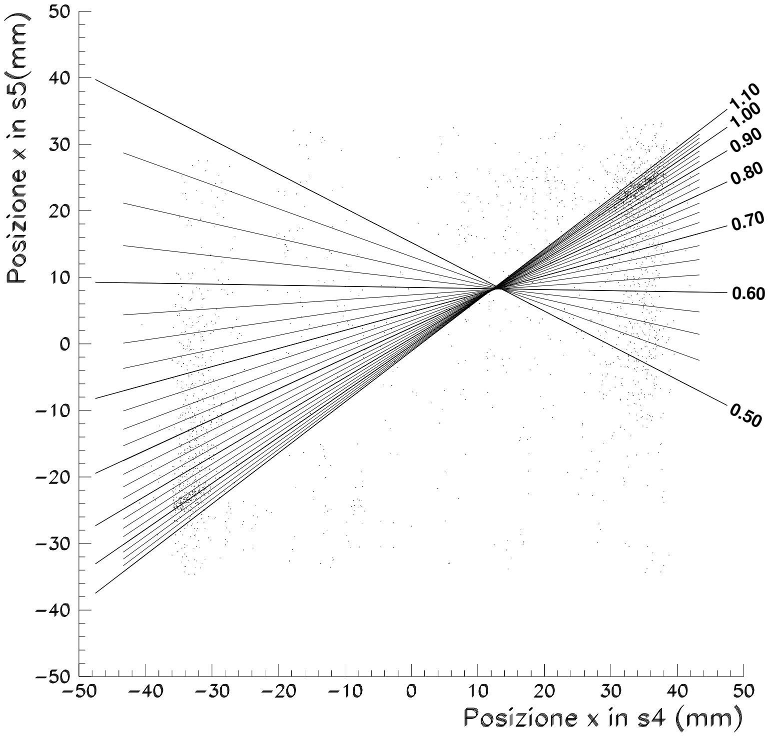

y projection:
better resolution,
ambiguity

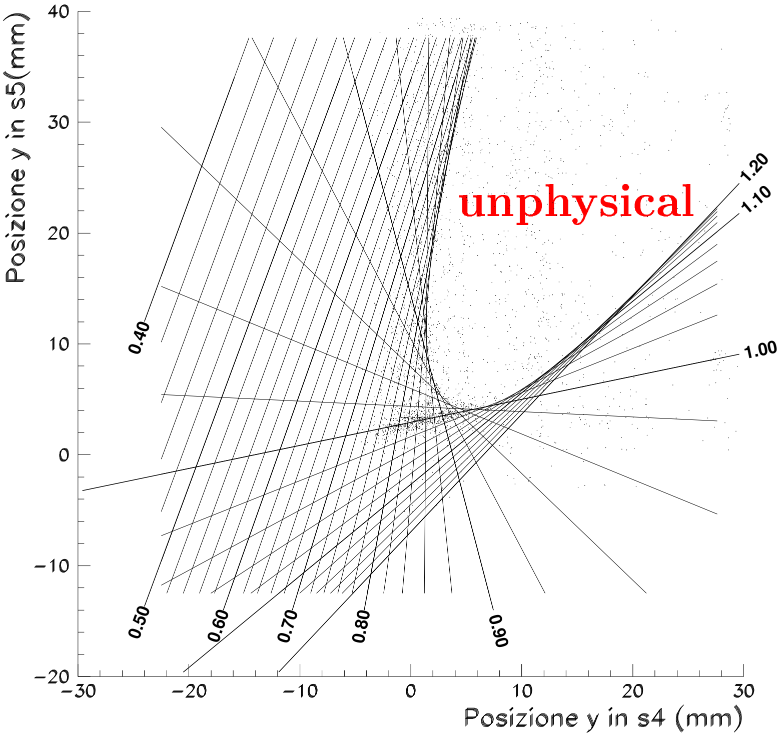

The LPS Reconstruction

The mometum x_L is evaluated using fast look-up tables.

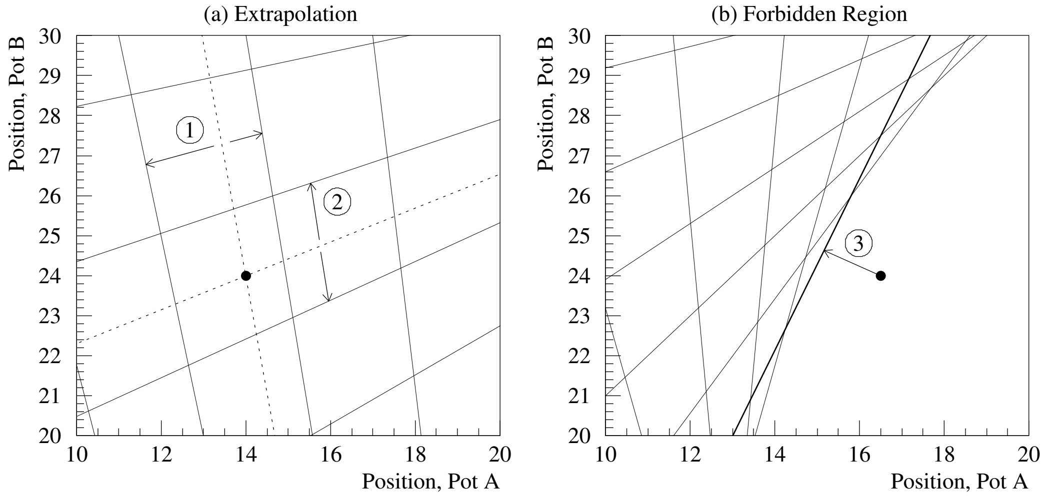

Once x_L is determined, p_T is obtained by **T** matrix inversion.

Track fit

5 parameters $(p_x, p_y, p_z, x_0, y_0)$ track fit with constrain to the I.P.

Also returns:

1. χ^2 and n.d.o.f.;
2. $P_m = \prod_{missing} (1 - \epsilon_i)$;
3. Δ_{pipe}, minimum distance to beam-pipe wall.

$\Rightarrow$ Reconstruction efficiency $> 90\%$

$\Rightarrow$ Resolution

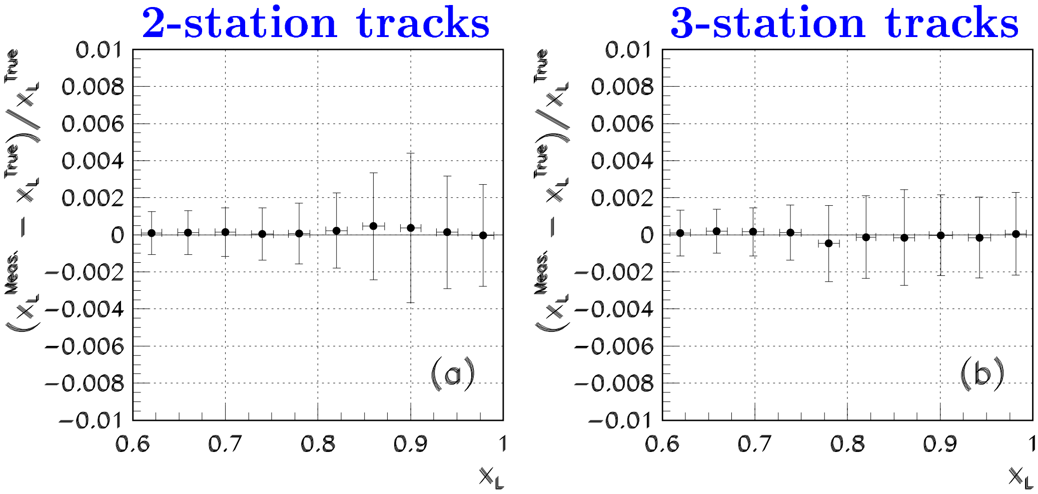

$\sigma_{x_L}/x_L \simeq$ **0.3%** at $x_L = 1$

$\sigma p_T \ll$ **90 MeV** (beam p_T spread)

$\sigma_{v_X} \simeq 350\ \mu m$

$\sigma_{v_Y} \simeq 80\ \mu m$

The LPS Alignment

Difficult ! Key values for the reconstruction are:

- **magnetic field of 23 beam elements** (known with good accuracy)
- **position of quadrupole axes**
- **position of detector strips** (parametrized as *strip equations*)
- **vertex position and beam tilt at the I.P.**
- **position of beam apertures**

Method: use tracks (x_L is a-priori unknown !!)

- align the detectors planes within each station
- align stations S5,S6 relative to S4 (use $x_L = 1$ kinematic peak)
  $\Rightarrow$ calculate proton momentum from 3-station tracks
- fit the LPS spectrometer position relative to ZEUS with

$$\chi^2 = \sum_{i=1}^{n} \left(\frac{(xv_{LPS} - xv_{CTD})}{\sigma_x} \right)^2 + \left(\frac{(yv_{LPS} - yv_{CTD})}{\sigma_y} \right)^2$$

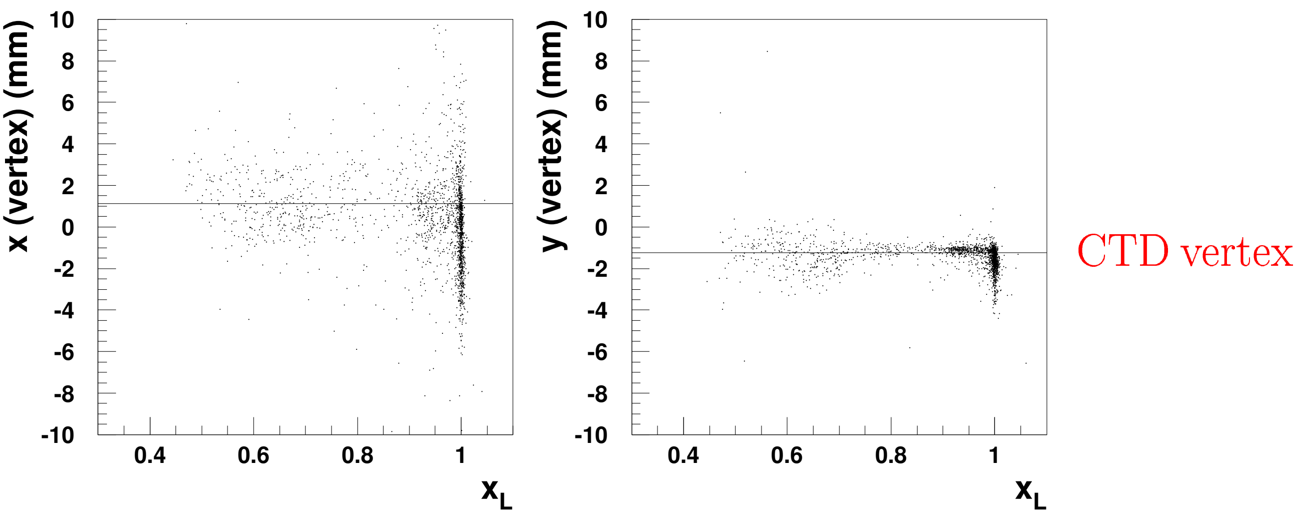

LPS vertex distribution

- Use coincidence S1 with S4→S6 to fix S1→S3 position.

The p_T Calibration

choose a set of elastic ρ° photoproduced $(\gamma p \to \rho^0 p)$
(line $x_L = 1$ spectrum; $\Delta(x_L) \simeq 10^{-4}$)
$\Rightarrow \theta_x = p_{x\rho^0} + p_{xp}; \; \theta_y = p_{y\rho^0} + p_{yp}$

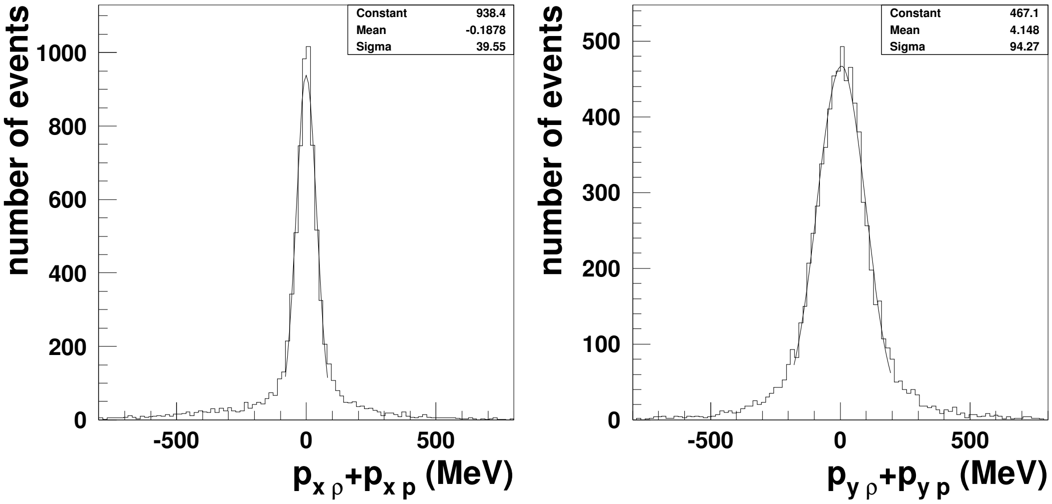

proton beam spread $\sigma_{p_x} \approx 40MeV$, $\sigma_{p_y} \approx 90MeV$

x_L resolution

$\frac{\sigma_{x_L}}{x_L}$(s4→s6)∼0.4%

$\frac{\sigma_{x_L}}{x_L}$(s1,s2)∼2%

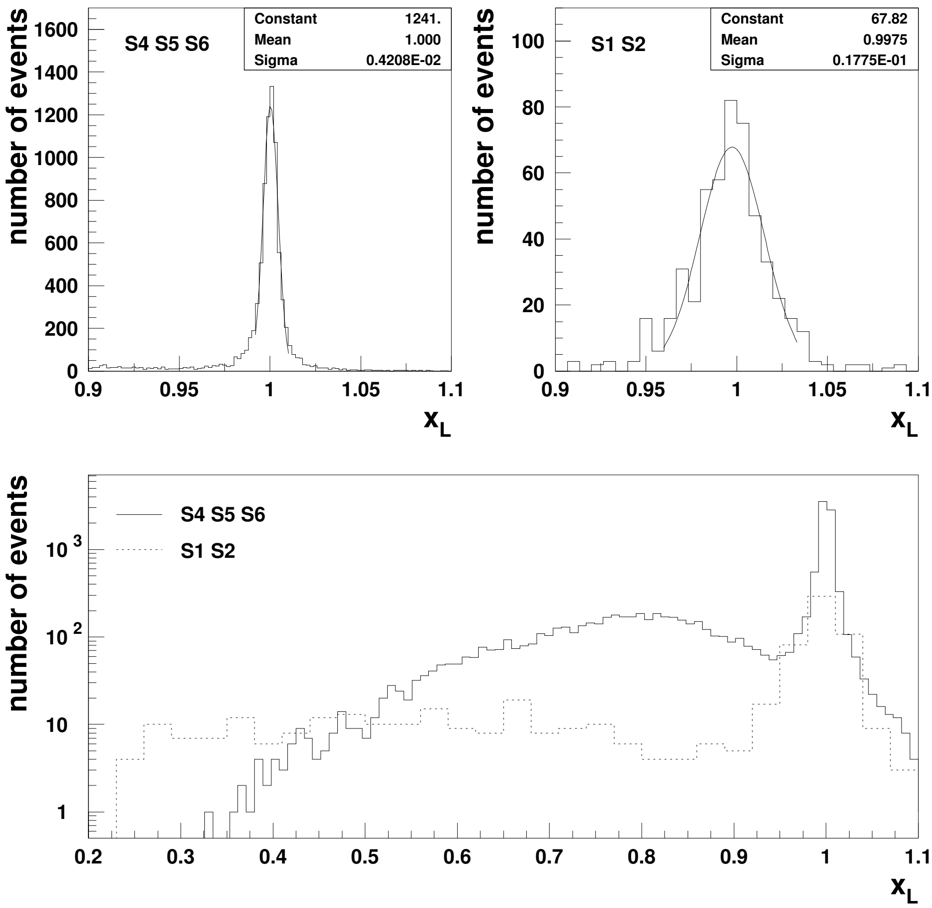

Location of beampipe apertures

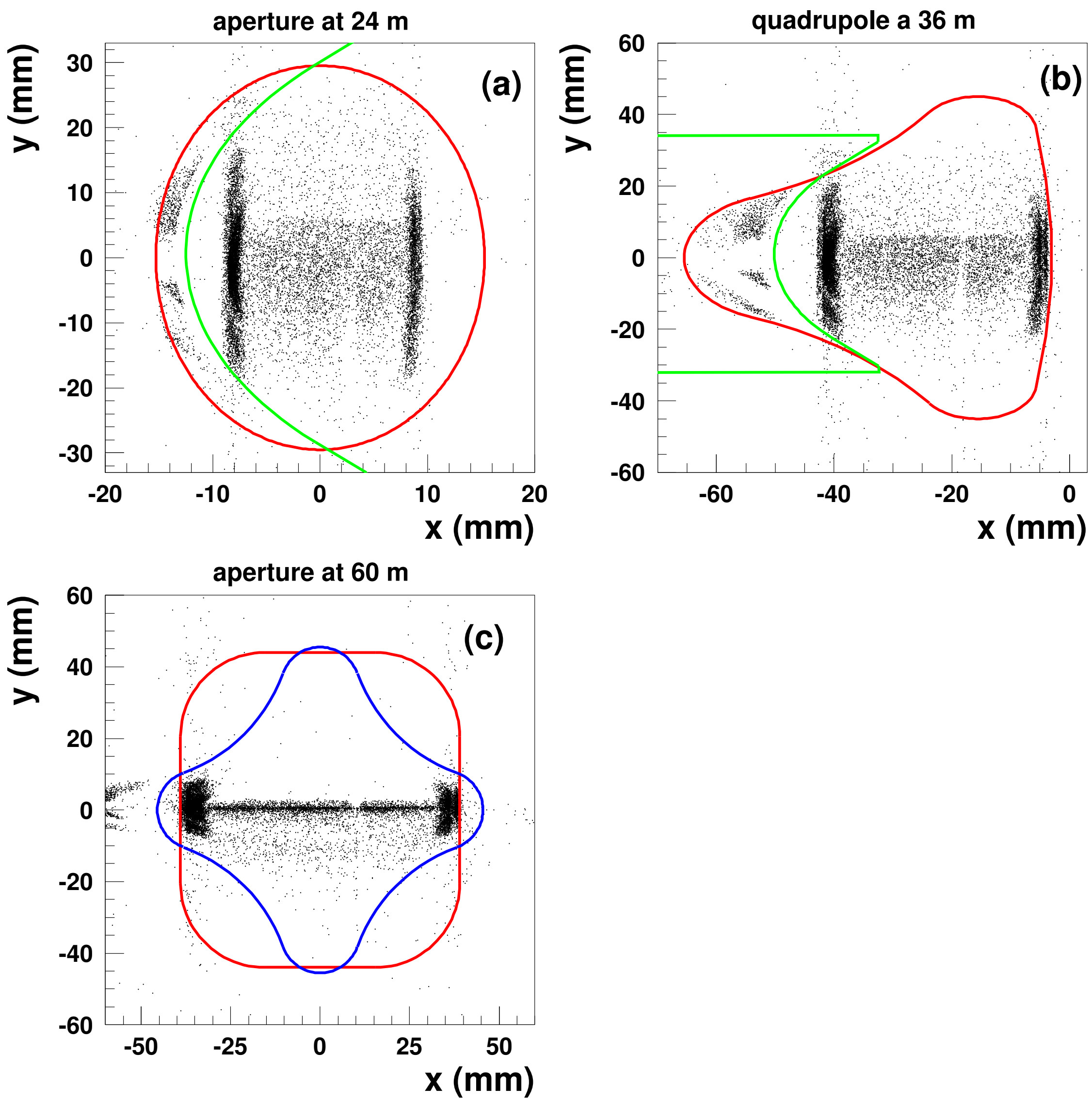

Position of beam pipe elements is cross-checked using reconstructed tracks.

Precision od the method: $\approx$ 200 μm

Acceptance sensitivity reduced by requiring $\Delta_{pipe} > 0.5$ mm

LPS ACCEPTANCE

1994 data taking (only S4→S6)

different p_T^2 distributions

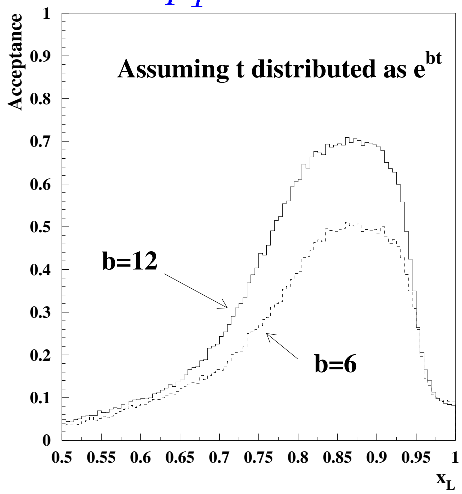

ACCEPTANCE

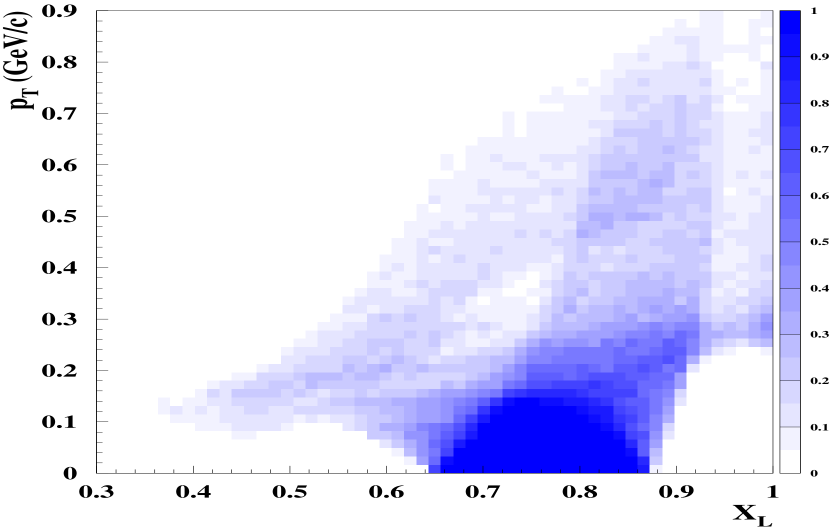

Acceptance ε at $x_L = 1$

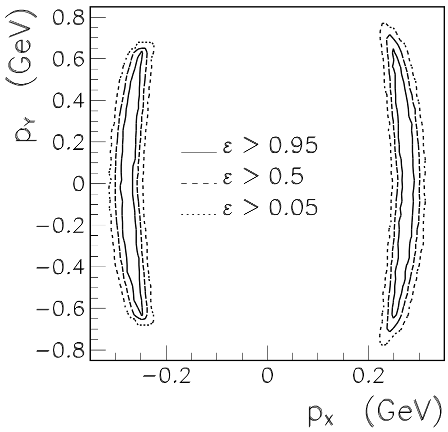

On average: $\varepsilon \simeq 3-6\%$ (diffractive)

$\varepsilon \simeq 20\%$ (low x_L)

ACCEPTANCE EXTENSION

Since 1995 (S1→S3 added)

(unfavoured with e^+ beams)

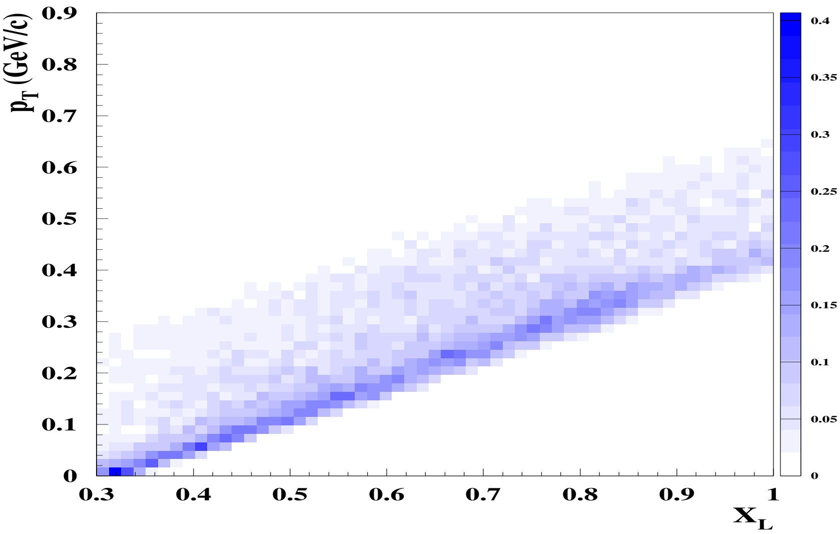

LPS ACCEPTANCE (cont'd)

Accepted phase space for **any coincidence of 2 stations** in S4→S6

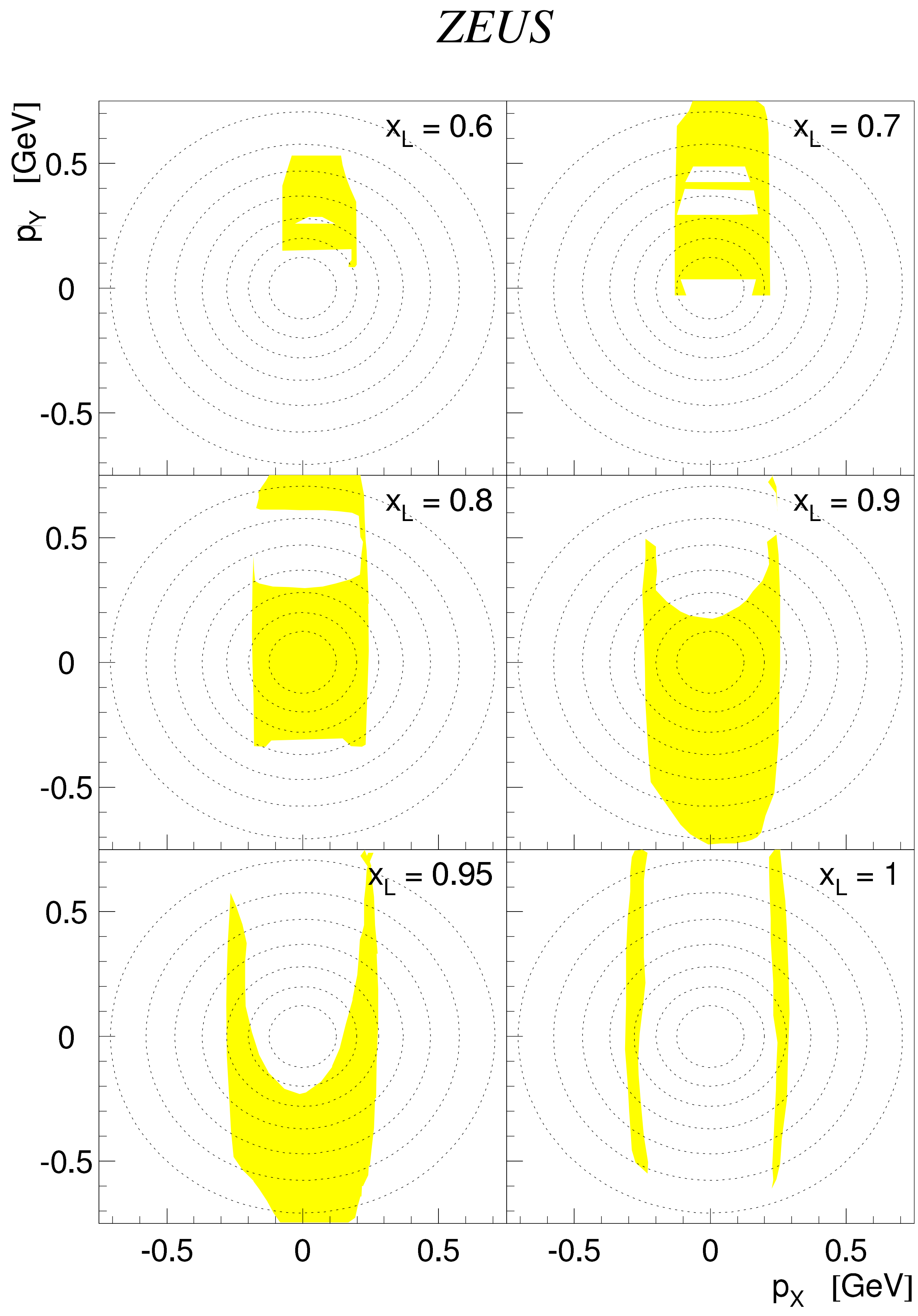

The η_{MAX}–x_L plane

η_{MAX} = pseudorapidity of the most forward energy deposit.

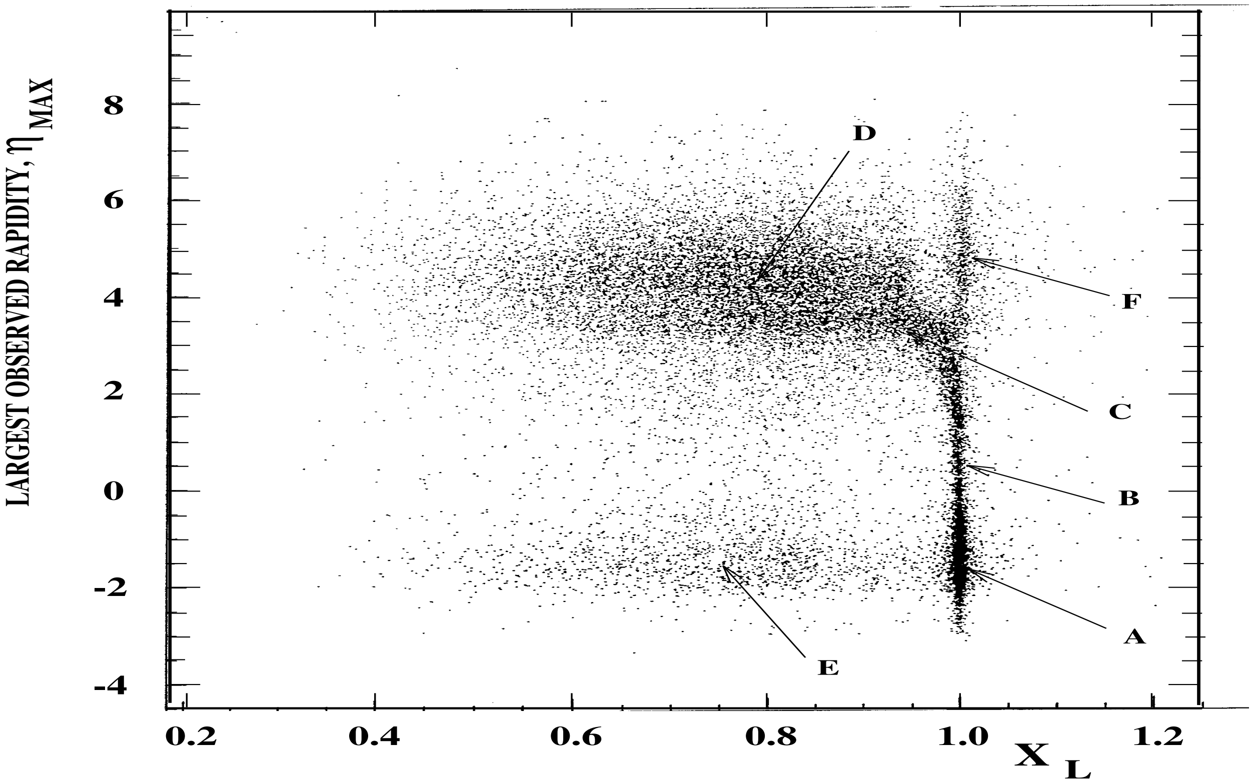

A–B Main diffractive group.
A rapidity gap is observed in the central detector.

C The band curves to lower x_L.
high η_{MAX} → massive states → lower x_L

$$M_x \propto \sqrt{1 - x_{Bj} - x_L}$$

D η_{MAX} saturates (forward beam pipe hole).

E $x_L = 1; \eta_{MAX} \geq 4$ → coincidence of beam halo track and central detector activity.

F A rapidity gap is observed together with a low energy proton. ⇒ proton diffractive dissociation.

Selection methods for diffraction

- Require a leading proton of fractional momentum $x_L = p'/p \simeq 1$

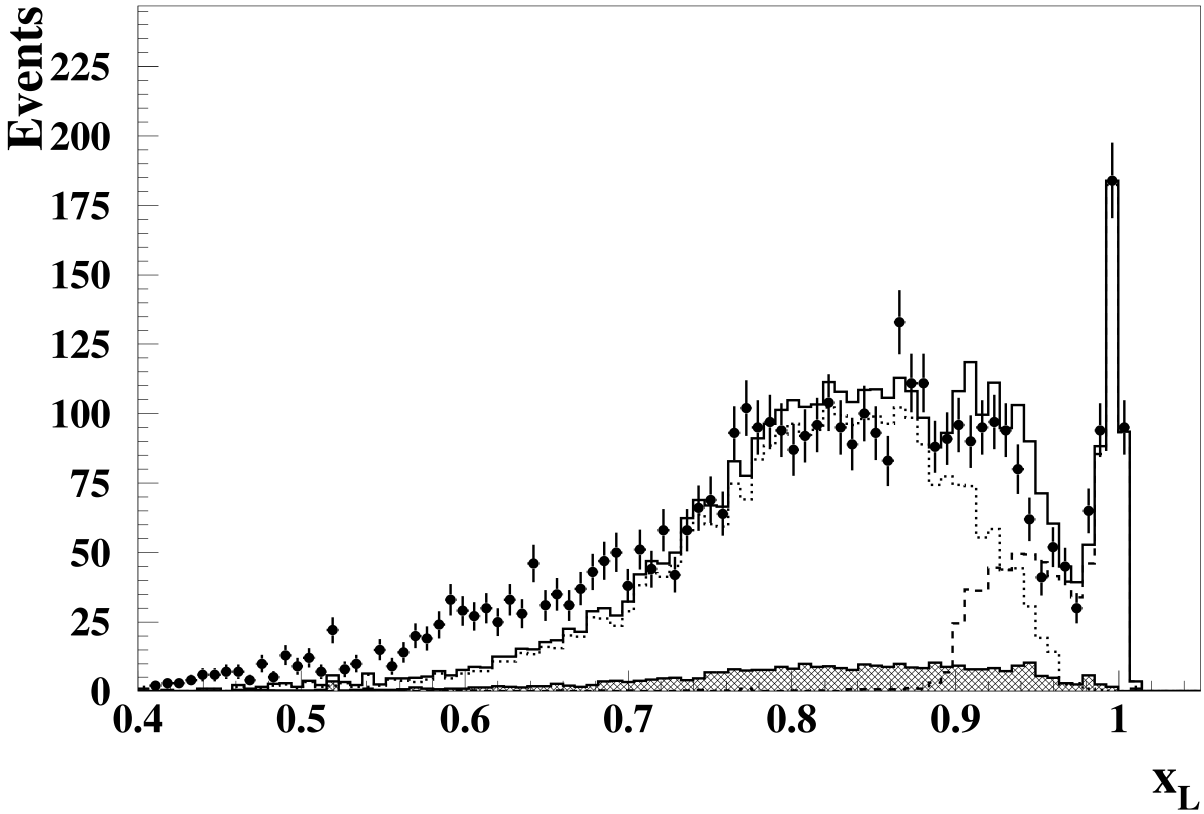

Diffractive analyses using the LPS allow

⇒ **clean selection of single diffraction (back. $\lesssim$ 10%)**

⇒ **measurement of t in the inclusive reactions**

⇒ **access higher diffractive masses ($M_X \lesssim 35$ GeV)**

⇒ **better constrain the kinematics.**

Problem: limited acceptance ⇒ limited statistics

The beam halo background

Mostly $x_L \sim 1$ protons $\Longrightarrow$ fake diffractive signal!

Consider the conserved quantity $(E + p_z)$:

$$2E_p = 1640 \text{ GeV} = (\mathrm{E} + \mathrm{p_z})^{\mathrm{in}}$$
$$\simeq 2E'_p + (E + p_z)_{Cal}$$

Halo events appear to violate energy/momentum conservation

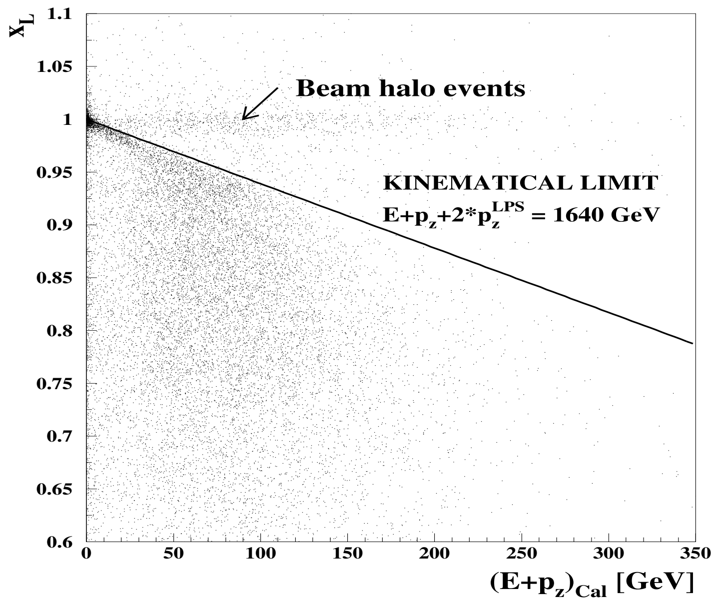

The $(E+p_z)$ distribution is a sum of good coincidence and random coincidence events.

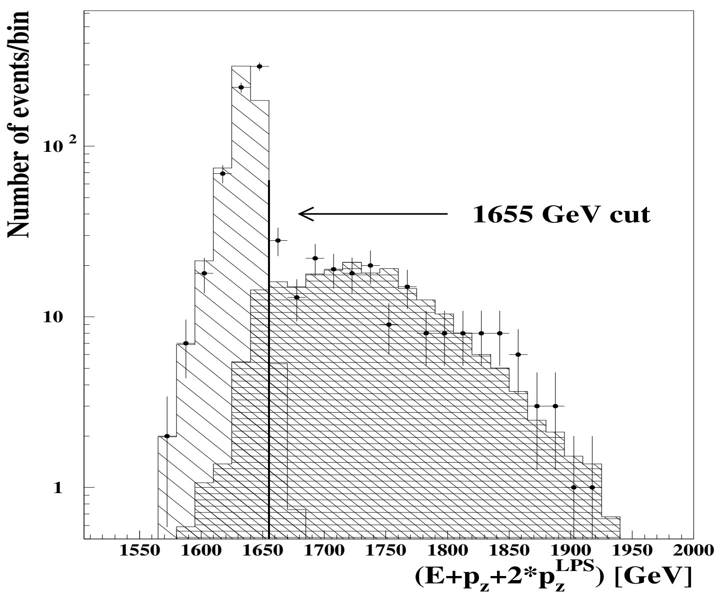

Cut $(E + p_z) < 1655$ GeV to reject beam halo.

Residual background estimated by randomly mixing $(E + p_z)_{Cal}$ and E'_p of tagged halo protons and fitting to the observed $(E + p_z)$ distribution.

Assuming halo uncorralated with the main detector activity:

$$\varepsilon_{halo} = 0.25 \pm 0.03 \ \%$$

Halo background left after the cut is normally ≈ 5 %

Note: Larger halo-background starting in 1996 $\Rightarrow$ HERA-B

Measurement of t

The value of t can be directly measured from the proton:

$$t = (p - p')^2 \approx -\frac{p_T^2}{x_L}[1 + (m_p^2/p_T^2)(x_L - 1)^2]$$

$$\approx -p_T^2 \quad \text{(for } x_L \sim 1\text{)}$$

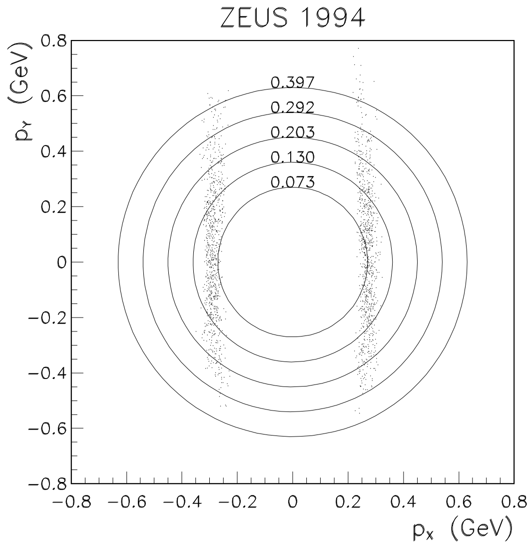

The resolution on the measurement is affected by intrinsic beam p_T spread due to the beam emittance

$$\sigma_{p_x} \simeq 40 \text{ MeV} \quad ; \quad \sigma_{p_y} \simeq 90 \text{ MeV}$$

⇒ t resolution ≈ 20 %

Extraction of the b slope

Fit t distribution to an exponential

$$\frac{d\sigma}{dt} = A \cdot \exp(-b|t|)$$

Large migration low → high t

⇒ correct by unfolding

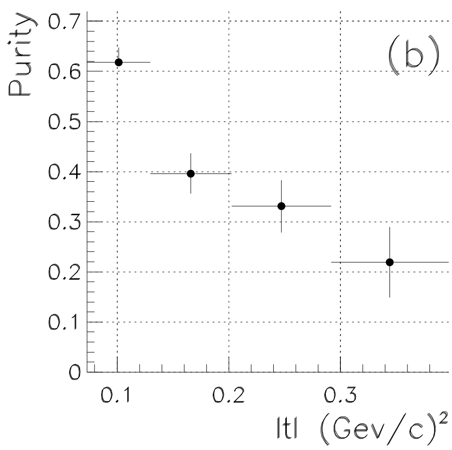

Fit p_T^2 distribution to the convolution of an exponential and a 2-D gaussian

$$\frac{d\sigma}{p_T^2} = \pi B(\sigma_{p_x}^2, \sigma_{p_y}^2) \exp\left\{b[1 - (\sigma_{p_x}^2 + \sigma_{p_y}^2)b]p_T^2\right\} \cdot I_o\left[(\sigma_{p_y}^2 - \sigma_{p_x}^2)b^2 p_T^2\right]$$

Note on diffractive mass (M_X) reconstruction

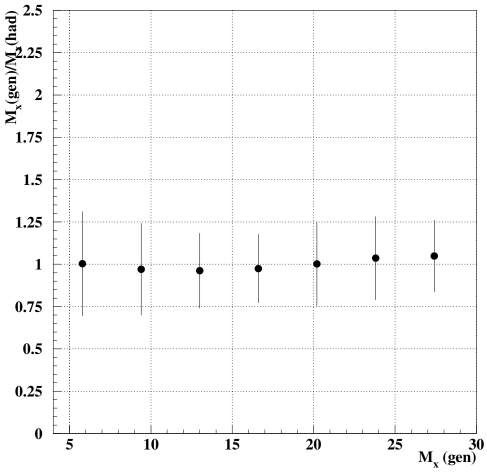

using the hadronic system

$$M_{had}^2 = (\Sigma_h E^h)^2 - (\Sigma_h p_X^h)^2 - (\Sigma_h p_Y^h)^2 - (\Sigma_h p_Z^h)^2$$

- resolution $\sigma(M_{had}^2)/M_{had}^2 \sim 1/\sqrt{M_{had}}$
- correction factor for dead material ~ 1.25

using the proton and the electron

$$M_{LPS}^2 = (1 - x_L)(W^2 + Q^2 - m_p^2) - Q^2 + t$$

$$W^2 = s[1 - \frac{E_e'}{2E_e}(1 - cos\theta)]$$

- resolution $\sigma(M_{LPS}^2)/M_{LPS}^2 \sim \sigma_{x_L}/(1 - x_L)$
  - $\Rightarrow$ poor at low M_X
  - $\Rightarrow$ comparable to M_{had} for $M_X \gtrsim 10$ GeV
- no correction factor needed

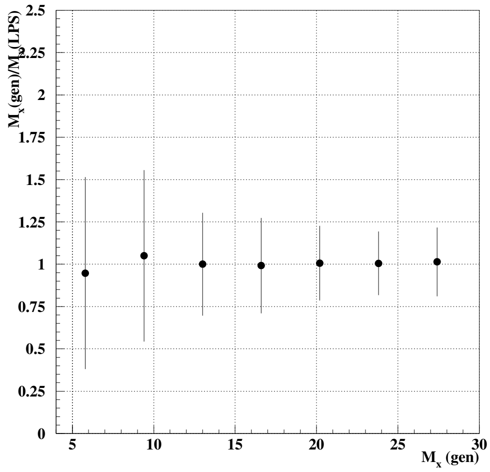

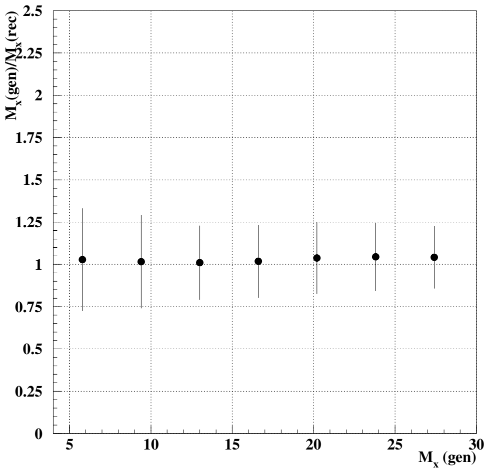

the 2 methods can be combined:

e.g. weighted average

$$M_X^2 = \frac{\frac{(M_{LPS})^2}{\sigma^2_{(M_{LPS})^2}} + \frac{(M_{had})^2}{\sigma^2_{(M_{had})^2}}}{\frac{1}{\sigma^2_{(M_{LPS})^2}} + \frac{1}{\sigma^2_{(M_{had})^2}}}$$

CONCLUSIONS

- **The LPS has been the first roman pot system installed an operated at HERA since 1993**
  - ⇒ $\sim$ **54000 readout channels**
  - ⇒ **fast (10 MHz) FE VLSI electronics and trigger capabilities**
  - ⇒ **automatic pot operations from ZEUS control room**
  - ⇒ **efficiency $\sim$ 60% depending on beam quality:**
    $\sim$ 70 pb^{-1} total integrated luminosity

- **A special reconstruction method was developed to maximize the acceptance**
  - ⇒ **use 2 stations + I.P.**
  - ⇒ **reconstruction efficiency $>$ 90 %**

- **Alignment and calibration was performed using tracks**
  - ⇒ **diffractive physics provides a bright calibration line**
  - ⇒ **elastic photoproduced ρ° used to calibrate p_T**
  - ⇒ **resolution ($\Delta x_L/x_L \simeq 0.4\%$) at $x_L = 1$ achieved;**
    p_T resolution limited by beam spread

Although limited by statistics, the LPS offers a wide range of applications.

Specific to diffraction:

- **A very clean tag for diffractively produced states, both for low and high M_X.**
- **Direct and independent measurement of t in diffractive VM production, only possible t measurement for inclusive photoproduction and DIS.**
- **Indirect measurement of the diffractively produced mass M_X by missing mass method for $M_X > 6$ GeV.**
- **In diffractive VM production, a clean tag for proton dissociation.**